Stimulus-dependent differential regulation in the *Escherichia coli* PhoQ–PhoP system

Tim Miyashiro* and Mark Goulian*†‡

Departments of *Physics and †Biology, University of Pennsylvania, Philadelphia, PA 19104

Edited by Bonnie L. Bassler, Princeton University, Princeton, NJ, and approved August 20, 2007 (received for review January 2, 2007)

In *Escherichia coli*, *Salmonella*, and related bacteria, the PhoQ–PhoP system regulates the expression of a large collection of genes in response to conditions of low magnesium or to the presence of certain antimicrobial peptides. We measured transcription of four PhoP-regulated promoters in *E. coli* that have significantly different PhoP-binding sites. Surprisingly, three promoters show identical responses to magnesium concentrations that range over four orders of magnitude. By analyzing and testing a simple model of transcriptional regulation, we find an explanation for this puzzle and show that these promoters are indeed differentially regulated at sufficiently high levels of stimulus. We then use this analysis to infer an effective level of phosphorylated PhoP as a function of magnesium stimulus. Our results demonstrate that differential regulation generally depends on the strength of the stimulus and highlight how quantitative analysis of stimulus–response curves can be used to infer properties of cell regulatory circuits that cannot be easily obtained from *in vitro* measurements.

modeling | response regulator | single cell fluorescence | two-component signaling

In bacteria, a collection of genes controlled by a common regulatory network often show considerable diversity in expression patterns. In many cases, this differential regulation can be explained by combinatorial control by multiple transcription factors or by the action of a single transcription factor that functions as both an activator and a repressor. However, an additional and more subtle form of differential regulation can arise for a group of genes when a transcription factor has significantly different binding affinities for the various promoters. In this case, increasing concentrations of the transcription factor can lead to an ordering or hierarchy of transcriptional activation. Such differential regulation has been suggested to play a critical role in cellular processes that require temporal control, as in the synthesis of complex molecular assemblies, or that depend on the strength or type of input stimulus (e.g., refs. 1–5).

The PhoQ–PhoP two-component signaling system, which is found in *Escherichia coli*, *Salmonella*, and related bacteria, is an example of a regulatory circuit that controls expression of a large collection of genes (6–9). PhoQ is a histidine kinase that phosphorylates its cognate response regulator PhoP in response to low extracellular levels of magnesium and to the presence of some antimicrobial peptides (6, 10–13). Phosphorylated PhoP (PhoP-P) functions as a regulator of genes associated with magnesium transport, outer-membrane modification, acid resistance, and pathogenesis (6–9, 14–17).

Recent *in vitro* studies of several promoters regulated by PhoQ–PhoP in *E. coli* identified specific PhoP-binding sites termed PhoP-boxes (7, 18). Furthermore, PhoP binds some of these promoters with significantly different affinities. As a result, these PhoP-regulated promoters may be differentially regulated *in vivo* so that with increasing levels of PhoQ stimulation, promoters with high-affinity binding sites are activated first, followed by promoters with progressively lower affinity sites. To explore this possibility, we used two-color fluorescent reporter strains to measure stimulus–response curves of several PhoQ–PhoP regulated genes with a high level of precision. Surprisingly, we did not observe differential regulation over a large range of stimulus (magnesium concentration) for several promoters, despite the variations among their PhoP-box sequences and the significant differences in PhoP-binding affinity *in vitro*. By analyzing a simple model of transcriptional regulation and testing predictions of this model, we find an explanation for this puzzle and show that these promoters are indeed differentially regulated at sufficiently high levels of stimulus. Interestingly, we find that the order of promoter activation *in vivo* is qualitatively different from the order expected from *in vitro* measurements. We also use our analysis to infer an effective level of phosphorylated PhoP as a function of magnesium stimulus.

Results and Discussion

The Transcription Profiles in Response to Mg^{2+} Stimulus Are Indistinguishable for Several PhoP-Regulated Genes. To study differential regulation in the PhoQ–PhoP system, we constructed a set of isogenic, two-color fluorescent reporter strains for four promoters (*mgtA*, *phoPQ*, *mgrB*, and *hemL*) that have markedly different binding affinities for PhoP. Each reporter strain contains *yfp*, the gene for yellow fluorescent protein (YFP), under the control of a particular PhoP-regulated promoter, and *cfp*, the gene for cyan fluorescent protein (CFP), under the control of a constitutive promoter (Fig. 1*a*). In the experiments described below, CFP fluorescence serves as an internal reference level for measuring YFP fluorescence in individual cells. This controls for variations in YFP due to extrinsic variability in gene expression (19, 20), variability in experimental measurements, and variations in total protein levels for different culture conditions (21, 22). As a result, the YFP/CFP fluorescence ratio provides a remarkably precise measurement of transcriptional activity as a function of stimulus.

The PhoQ–PhoP two-component system is stimulated under conditions of low extracellular magnesium (23–25). Indeed, the steady-state YFP/CFP fluorescence ratio of each reporter strain increased with decreasing concentrations of magnesium (Fig. 1*b*). The magnesium concentration that results in the half-maximal transcriptional response to Mg^{2+} ($[Mg^{2+}]_{50\%}$) was highest for the *mgtA* promoter (Fig. 1*c*), which also has the highest affinity for PhoP *in vitro* (7). However, the values of $[Mg^{2+}]_{50\%}$ for the *mgrB*, *phoPQ*, and *hemL* promoters were not significantly different from each other (Fig. 1*c*). This suggests that the Mg^{2+} response curves in Fig. 1*b* corresponding to these three promoters are the same, after compensating for the basal and maximal levels of transcription at high and low magnesium,

Author contributions: T.M. and M.G. designed research; T.M. performed research; T.M. and M.G. analyzed data; and T.M. and M.G. wrote the paper.

The authors declare no conflict of interest.

This article is a PNAS Direct Submission.

Abbreviations: PhoP-P, phosphorylated PhoP; YFP, yellow fluorescent protein; CFP, cyan fluorescent protein.

‡To whom correspondence should be addressed at: Department of Biology, 433 South University Avenue, Philadelphia, PA 19104-6018. E-mail: goulian@sas.upenn.edu.

This article contains supporting information online at www.pnas.org/cgi/content/full/0700025104/DC1.

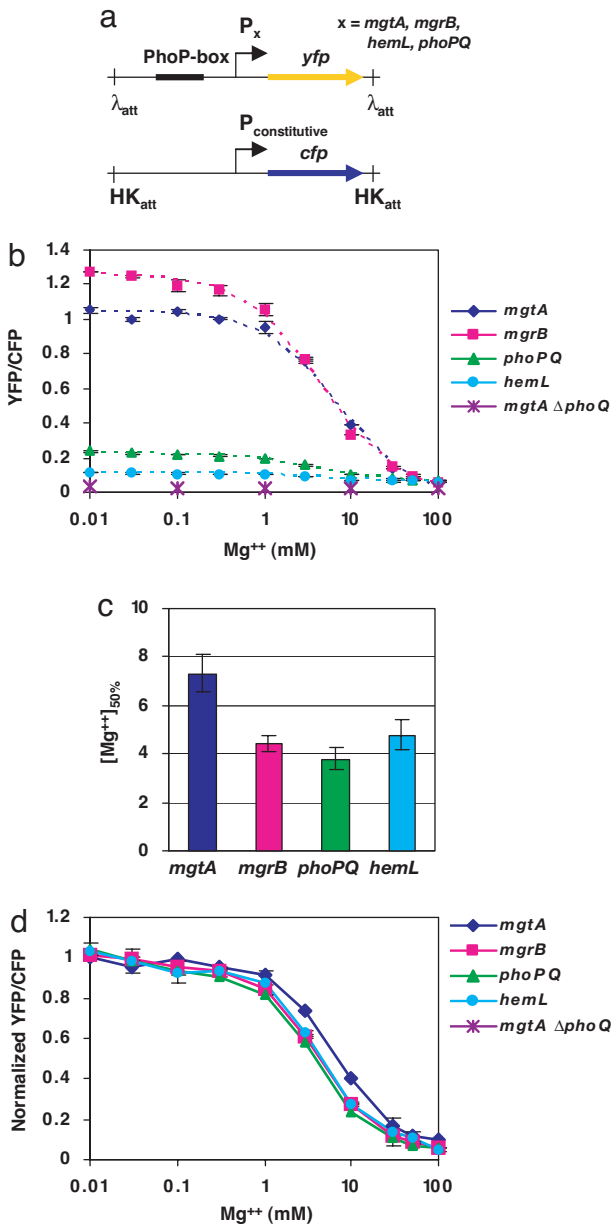

Fig. 1. Transcription profiles of four PhoP-regulated promoters in response to extracellular [Mg^{2+}]. (*a*) Each reporter strain contains a chromosomal copy of *yfp* controlled by a PhoP-regulated promoter, and a copy of *cfp*, controlled by a constitutive promoter (*tetA* promoter), at the attachment sites of λ and HK022 phages, respectively. The expression of CFP from the *tetA* promoter is constant over the range of magnesium concentrations used in our experiments (22). (*b*) Steady-state transcription of PhoP-regulated promoters as measured by the YFP/CFP fluorescence ratio of single cells. Cultures were grown at 37°C in minimal medium containing the indicated concentrations of $MgSO_4$. Each point indicates the mean of two independent cultures, and each bar indicates the corresponding range. The dotted lines denote fits to saturating curves. (*c*) Concentration of magnesium at which YFP/CFP is halfway between the maximal and minimal values, determined for each promoter from the fitted curves in *a*. Bars denote the errors from the nonlinear fits. (*d*) Normalized curves from *b*. Each curve was normalized by shifting and rescaling by constants. For details of the analysis, see *SI Text*.

respectively. To check this, we normalized the curves by shifting and rescaling so that they coincide at regions of high and low Mg^{2+} [for details, see supporting information (SI) *Text*]. After normalization, the Mg^{2+} response curves of the *mgrB*, *phoPQ*, and *hemL* reporter strains were indistinguishable (Fig. 1*d*). This result was not due to the particular method of constructing the reporters because an operon fusion of *yfp* to *mgrB* at its wild-type locus showed the same normalized curve as the *mgrB* promoter reporter (SI Fig. 5). In addition, the normalized Mg^{2+} response curve for the *mgtA* promoter did not overlap with the corresponding curves for the *mgrB*, *phoPQ*, or *hemL* promoters (Fig. 1*d*). Under identical growth conditions, the four reporter strains should have the same intracellular concentration of PhoP-P ([PhoP-P]). Therefore, our results suggest that the normalized transcriptional responses of the *mgrB*, *phoPQ*, and *hemL* promoters to [PhoP-P] are indistinguishable in cells grown under the steady-state conditions described in Fig. 1.

We did not observe a hierarchy of transcriptional activation among all four PhoP-regulated promoters in response to different levels of magnesium. In fact, three of the promoters showed the same transcriptional profile. One possible explanation for this striking result is that PhoP-P has identical binding affinities at the *mgrB*, *phoPQ*, and *hemL* promoters *in vivo*. However, this seems unlikely because the sequences of the PhoP-boxes are substantially different (see Fig. 3*a*) and PhoP binds the promoters with different affinities *in vitro* (7) (SI Fig. 6). Furthermore, the results described below suggest that the *in vivo* binding affinities of PhoP-P for the three promoters are indeed different. An alternative explanation is that the level of PhoP-P remains below the *in vivo* PhoP-P dissociation constants for the *mgrB*, *phoPQ*, and *hemL* promoters throughout the range of [Mg^{2+}] in Fig. 1*b*. For this range of [PhoP-P], the fractional occupation of these promoters by PhoP-P will be proportional to [PhoP-P] (or proportional to a power of [PhoP-P] for the case of cooperative binding). Furthermore, if we assume that transcriptional activation of a PhoP-regulated promoter is proportional to the fractional occupation by PhoP-P, then the normalized transcription profiles as a function of [PhoP-P] (or equivalently [Mg^{2+}]) will be indistinguishable for the *mgrB*, *phoPQ*, and *hemL* promoters. The distinct behavior of the *mgtA* promoter can then be attributed to a significantly lower PhoP-P binding constant. These points are illustrated in Fig. 2 and are tested experimentally below.

In the above analysis and in what follows, we have made the simplifying assumption that a single molecule of PhoP-P binds to a PhoP-regulated promoter. However, the conclusions are similar for the cases of binding by a PhoP-P dimer or of cooperative binding.

The Differential Regulation of *mgtA* Relative to *mgrB*, *phoPQ*, and *hemL* Is Associated with the *mgtA* PhoP-Binding Site. If PhoP-P levels in cells grown under the Mg^{2+} conditions described in Fig. 1 are well below the dissociation constants of the *mgrB*, *phoPQ*, and *hemL* promoters, then our model predicts that the fold change in transcription corresponding to a change in [Mg^{2+}] within this range will be the same for these promoters (see Fig. 2*c*). Consistent with the results in Fig. 1 and our model, we found that the fold increase in transcription from 10 mM to 100 μM [Mg^{2+}] was comparable for *mgrB*, *phoPQ*, and *hemL* (Fig. 3*b*). In contrast, *mgtA* showed a significantly lower fold increase (Fig. 3*b*), which suggests that [PhoP-P] at 100 μM [Mg^{2+}] is comparable to or greater than the dissociation constant for the *mgtA* PhoP-box, $K_{d,mgtA}$. To determine whether the distinct Mg^{2+} response of the *mgtA* promoter is associated with the PhoP-binding site, we similarly measured the fold increase in transcription for hybrid promoters in which the PhoP-boxes of the *mgrB* and *mgtA* promoters were swapped (Fig. 3 *a* and *c*). The hybrid promoter constructed by replacing the PhoP-box in the *mgtA* promoter with the *mgrB* PhoP-box (hybrid 1) showed a fold increase in transcription that was identical with that of the *mgrB* promoter. The reciprocal hybrid, with the *mgtA* PhoP-box replacing the *mgrB* PhoP-box in the *mgrB* promoter (hybrid 2), showed a fold increase in transcription that was intermediate

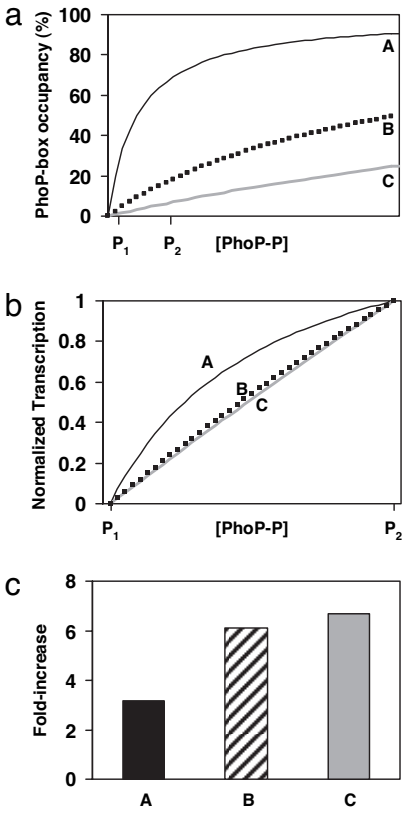

Fig. 2. A comparison of hypothetical PhoP-P binding curves and normalized transcription profiles for three promoters with different PhoP-P dissociation constants. (*a*) PhoP-P binding curves for three promoters (A, B, and C) with different dissociation constants. P_1 and P_2 denote [PhoP-P] at high and low [Mg^{2+}], respectively. In this study, we assume simple binding at these promoters; however, the conclusions of this analysis are the same for the cases of binding by a PhoP-P dimer or of cooperative binding. We also assume in this analysis that the rate of transcription for a particular promoter is a linear function of its fractional occupancy by PhoP-P. (*b*) The transcription profiles of the promoters in *a* normalized so that the transcription levels coincide at P_1 and P_2. The promoters with PhoP-P dissociation constants above P_2 (promoters B and C) have normalized transcription profiles that are essentially indistinguishable. In contrast, promoter A, which has a dissociation constant below P_2, has a distinct normalized transcription profile. (*c*) Fold increase in transcription from P_1 to P_2 for the promoters in *a*. Note that promoters with different PhoP-P dissociations constants greater than P_2 (promoters B and C) show the same fold increase. For details of the analysis, see *SI Text*.

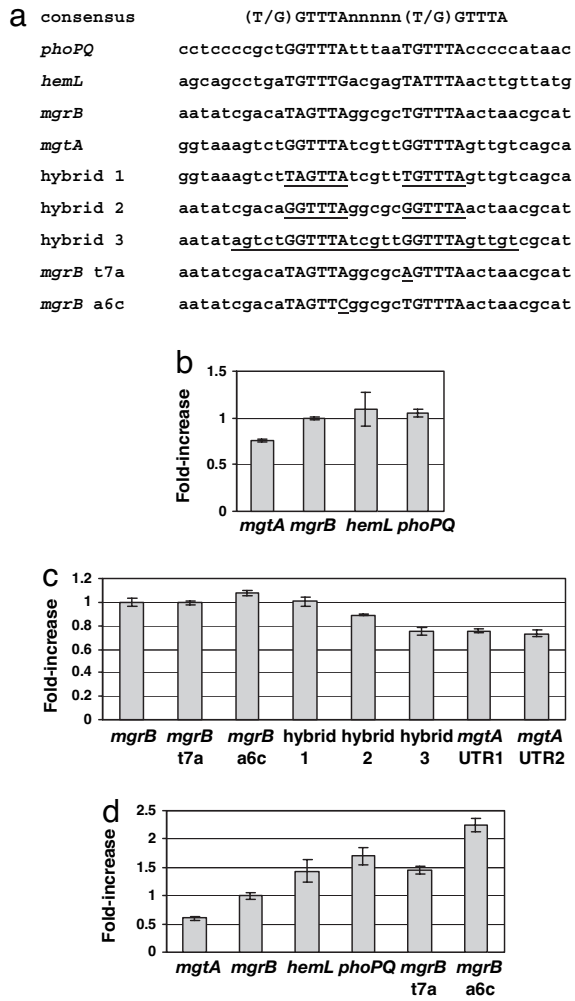

Fig. 3. Relative transcriptional activation for wild-type and mutated promoters. (*a*) Sequences of the consensus PhoP-box, the PhoP-boxes of the wild-type promoters, and the PhoP-boxes of the mutated promoters. Hybrid 1 consists of the *mgtA* promoter with the *mgrB* PhoP-box. Hybrid 2 and hybrid 3 consist of the *mgrB* promoter with the *mgtA* PhoP-box and with portions of flanking *mgtA* sequence, respectively. (*b*) Fold increase in transcription of wild-type promoters (relative to the fold increase of *mgrB* transcription) for cells grown in 100 μM Mg^{2+} compared with 10 mM Mg^{2+}. Fold increase is defined to be the following: $[(YFP/CFP)_{100\ \mu M\ Mg^{2+}} - (YFP/CFP)_{100\ \mu M\ Mg^{2+},\Delta phoQ}]/[(YFP/CFP)_{10\ mM\ Mg^{2+}} - (YFP/CFP)_{10\ mM\ Mg^{2+},\Delta phoQ}]$. (*c*) Fold increase as in *b* for several mutated promoters listed in *a*. Two different versions of the *mgtA* reporter are also compared. UTR1 has the native 5′-UTR for *mgtA*, which includes a potential riboswitch. UTR2 has a truncated 5′-UTR with only 16 base pairs of the original 263 base pairs in the *mgtA* 5′-UTR. (*d*) Fold increase in transcription of various promoters (relative to the fold increase of *mgrB* transcription) for cells exposed to LL-37 in 100 μM Mg^{2+} for 1 h, compared with cells in 100 μM Mg^{2+} without LL-37. Fold increases were computed by using YFP/CFP values determined from two independent cultures. The bars denote estimates of the error determined from the corresponding ranges of the YFP/CFP measurements.

between those of the *mgrB* and *mgtA* promoters. A second hybrid *mgrB* promoter, which has a larger substitution of the PhoP-binding region from the *mgtA* promoter (hybrid 3), showed a fold increase in transcription that was identical with that of *mgtA*. These results provide further evidence that the differential regulation of the *mgtA* promoter, relative to the *mgrB*, *phoPQ*, and *hemL* promoters, is due to a lower PhoP-P dissociation constant for the *mgtA* PhoP-binding site. The results also suggest that additional sequences adjacent to the PhoP-box consensus sequence may play a role in determining PhoP-P binding affinity *in vivo* at some promoters.

A recent study has shown that a Mg^{2+}-responsive riboswitch within the 5′-UTR of the *mgtA* transcript contributes to magnesium regulation of *mgtA* expression in *Salmonella typhimurium* (26). Computer analysis suggested that the 5′-UTR of the *E. coli mgtA* transcript may also function as a riboswitch (26). Our *E. coli mgtA* reporter construct contains the native *mgtA* 5′-UTR (263 base pairs) upstream of the *yfp* start codon. However, a different *mgtA* reporter strain, which contains only 16 base pairs from the native *mgtA* 5′-UTR, exhibited the same response to Mg^{2+} (Fig. 3*c*). In addition, the hybrid 3 construct described above, which produces a transcript that completely lacks the *mgtA* 5′-UTR, showed the same response to Mg^{2+} as that of the *mgtA* promoter (Fig. 3*b*). If there is a riboswitch in the *mgtA* 5′-UTR in *E. coli*, our results suggest that it is not sensitive to the range of [Mg^{2+}] in our experiments.

The Mg^{2+} Response of the *mgrB* Promoter Is Insensitive to PhoP-Box Mutations That Weaken Transcription. If the levels of PhoP-P associated with the range of [Mg^{2+}] used in our experiments are

MICROBIOLOGY

well below the dissociation constant of a particular promoter, then mutations that decrease the PhoP binding affinity, i.e., raise the dissociation constant, should not affect the normalized transcriptional response to a change in $[Mg^{2+}]$. To test this, we weakened the *mgrB* promoter by mutating its PhoP-box. Two bases within the PhoP-box of the *mgrB* promoter that are also present within the consensus sequence were individually mutated (Fig. 3*a*). The YFP expression levels from the two mutated promoters were markedly attenuated compared with the corresponding level for the *mgrB* promoter (SI Fig. 7 *Left*). Nevertheless, for both promoters, the fold increases in transcription and the normalized Mg^{2+} response curves were comparable with the corresponding data for the wild-type *mgrB* promoter (Fig. 3*c* and SI Fig. 7 *Right*). Thus, consistent with the predictions of our model, weakening the *mgrB* PhoP-box does not affect the relative transcriptional response for $[Mg^{2+}]$ over the range 100 mM to 10 μM.

Stimulation of PhoQ with the Antimicrobial Peptide LL-37 Reveals Differential Regulation of *mgrB*, *phoPQ*, and *hemL*. The above results suggest that if the *mgrB*, *phoPQ*, and *hemL* promoters have significantly different PhoP-P dissociation constants, then differential regulation will emerge at sufficiently high levels of PhoP-P. However, such levels must be higher than those obtained for growth in 10 μM Mg^{2+}. We found that it was difficult to achieve steady-state growth conditions for magnesium concentrations <10 μM, presumably because the cells continually deplete the magnesium in the culture medium. We therefore used the antimicrobial peptide LL-37 to further stimulate PhoQ. LL-37 has been shown to activate the PhoQ–PhoP system in *S. typhimurium* (13). Similarly, for *E. coli* cells growing in 100 μM Mg^{2+}, the addition of LL-37 resulted in increased PhoP-regulated transcription (data not shown). Notably, the *mgrB*, *phoPQ*, and *hemL* promoters showed distinct transcriptional responses to LL-37 (Fig. 3*d*) in contrast with the indistinguishable Mg^{2+} responses described above (Fig. 3*b*). Thus, the increased PhoQ stimulation from exposure to LL-37 resulted in differential regulation of all four promoters.

The promoter with the highest fold increase in transcription was *phoPQ* (Fig. 3*d*), which suggests that the *phoPQ* promoter has the largest PhoP-P dissociation constant among the promoters tested in this study. Interestingly, this would provide maximal amplification of other PhoP-regulated promoters from *phoPQ* autoregulation before saturating PhoP production. However, this result is in striking contrast with the results from *in vitro* measurements that suggest the PhoP dissociation constant of the *phoPQ* promoter is lower than those of *mgrB* and *hemL* (see ref. 7 and SI Fig. 6). The *in vitro* measurements were made with unphosphorylated PhoP (see ref. 7 and *SI Text*). We were not able to produce sufficiently high levels of phosphorylated PhoP to perform the analogous *in vitro* measurements with PhoP-P. A previous study has shown that high-level expression of PhoP activates transcription of PhoP-regulated promoters independently of PhoQ or of phosphorylation (27). To determine whether overexpression of unphosphorylated PhoP leads to differential regulation of *mgtA*, *mgrB*, *phoPQ*, and *hemL* promoters, we overexpressed PhoP in Δ*phoQ* reporter strains. We found the differential regulation was similar to the *in vivo* results described above for $phoQ^+$ strains and in marked contrast with the *in vitro* PhoP binding measurements (SI Fig. 8). These results suggest that the observed differences between the *in vitro* and *in vivo* data are due to additional factors that affect PhoP binding affinity at PhoP-regulated promoters *in vivo* that are absent in the *in vitro* measurements.

Our model predicts that a promoter containing mutations that weaken the affinity of PhoP-P for its PhoP-box should also exhibit differential regulation, relative to the wild-type promoter, at sufficiently high levels of PhoP-P. To test this, we measured the transcriptional response to LL-37 for the *mgrB* promoters with either T7A or A6C substitutions in the PhoP-box (Fig. 3*a*). Both mutated promoters showed fold increases in transcription from stimulation with LL-37 that were above that of the wild-type *mgrB* promoter. These results are also consistent with the observation that the T7A substitution was the weakest of the three promoters: the T7A substitution showed the most attenuated Mg^{2+} response curve (SI Fig. 7 *Left*) and displayed the largest fold increase in transcription (Fig. 3*d*).

Taken together, the above results suggest that the *mgtA*, *phoPQ*, *mgrB*, and *hemL* promoters are differentially regulated under conditions that strongly stimulate the PhoQ–PhoP system (e.g., the presence of LL-37).

Effective PhoP-P Binding Curves. Within the context of our model, we can associate each transcription level of a PhoP-regulated promoter with a distinct value of [PhoP-P]. We call these values effective PhoP-P concentrations ($[PhoP\text{-}P]_{effective}$) because they are model dependent and may not reflect the actual concentrations of PhoP-P within the cell. Because $[PhoP\text{-}P]_{effective}$ should be the same in every reporter strain for a given growth condition, it provides a means to relate transcription levels of the PhoP-regulated promoters to each other. To extract a complete curve of transcription as a function of $[PhoP\text{-}P]_{effective}$ for a particular promoter, transcription measurements for sufficiently high levels of PhoQ stimulation such that the promoter approaches maximal binding to PhoP-P (saturated binding) are required. This will occur at PhoP-P concentrations well above the dissociation constant for the promoter (Fig. 2*a*). We were unable to observe saturation of any of the PhoP-regulated promoters studied here by varying either magnesium or LL-37 concentrations. Apparently, we were not able to reach sufficiently high levels of PhoP-P with either stimulus of PhoQ under our experimental conditions. Therefore, to reach higher levels of transcriptional activation, we used a constitutively active PhoP mutant, which we denote by $PhoP_{ca}$. When we expressed $PhoP_{ca}$ from an inducible promoter, we found that transcription from the *mgtA* promoter leveled off at high levels of induction, whereas transcription from the *mgrB*, *hemL*, and *phoPQ* promoters continued to increase (Fig. 4*a* and data not shown). This suggests that at the highest levels of $PhoP_{ca}$ reached in these experiments, the *mgtA* promoter is saturated.

By using this $PhoP_{ca}$-induction data and the model described in Fig. 2, we determined the curves of transcription as a function of $[PhoP\text{-}P]_{effective}$ for the *mgtA*, *mgrB*, and *hemL* promoters (Fig. 4*b*) (for details, see *SI Text*). Concentrations are expressed in units of $K_{d,mgtA}$, the dissociation constant of PhoP-P for the *mgtA* promoter. For the case of *mgrB*, the fit determined the dissociation constant for PhoP-P at the *mgrB* promoter to be $\approx 10K_{d,mgtA}$. For the *hemL* promoter, we found the range of $[PhoP\text{-}P]_{effective}$ resulting from expression of $PhoP_{ca}$ was too low to determine $K_{d,hemL}$. Although the curves in Fig. 4*b* were determined by using only $PhoP_{ca}$ expression data, the points corresponding to LL-37 stimulation (open symbols) are in good agreement.

From this analysis, we also inferred $[PhoP\text{-}P]_{effective}$ for cells grown in various concentrations of magnesium (Fig. 4*c*). These were separately determined from the YFP/CFP data for the *mgtA* and *mgrB* promoters (Fig. 1*b*). The two resulting curves are in close agreement (Fig. 4*c*). For the lowest magnesium level (10 μM $[Mg^{2+}]$), $[PhoP\text{-}P]_{effective}$ is well below the dissociation constant for *mgrB*, which is consistent with our conclusions above concerning the differential regulation of *mgrB* and *mgtA* promoters. This differential regulation is further illustrated in Fig. 4*d*, which shows the extent of PhoP-P binding to the two promoters (within the context of our model) as a function of magnesium. The dashed curves, which were determined from $PhoP_{ca}$ expression data (Fig. 4*b*), are in close agreement. These results suggest that the plateau in the Mg^{2+} response curves at

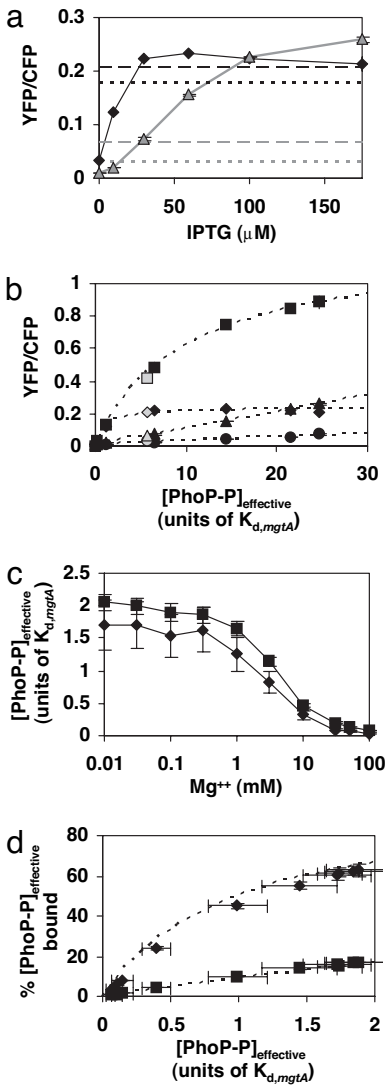

Fig. 4. Effective PhoP-P levels and resulting transcription and binding curves, inferred from the model of transcriptional activation described in Fig. 2. (*a*) Transcription of the *mgtA* (black diamonds) and *phoPQ* (gray triangles) promoters for various levels of $PhoP_{ca}$ expression. ($PhoP_{ca}$ is a constitutively active variant of PhoP.) Transcription levels corresponding to 100 μM [Mg^{2+}] and stimulation with LL-37 are indicated with dotted and dashed lines, respectively. The upper (lower) pair of dotted and dashed lines is for the *mgtA* (*phoPQ*) promoter. (*b*) Transcription of *mgrB* (squares), *mgtA* (diamonds), *hemL* (circles), and *phoPQ* (triangles) as a function of $[PhoP\text{-}P]_{effective}$. The filled symbols denote $PhoP_{ca}$ expression data, and the dotted lines are the associated fits. Note that the $PhoP_{ca}$ expression data for *phoPQ* fall on a line by construction. The open symbols denote transcription levels from stimulation with LL-37 in strains with wild-type *phoP*, which were not used in determining the fits. (*c*) $[PhoP\text{-}P]_{effective}$ as a function of [Mg^{2+}] determined from the transcription data in Fig. 1*b* for *mgtA* (diamonds) and *mgrB* (squares). (*d*) Inferred $[PhoP\text{-}P]_{effective}$ bound at the *mgtA* (diamonds) and *mgrB* (squares) promoters for cells grown in the levels of magnesium shown in Fig. 1*b*. The $[PhoP\text{-}P]_{effective}$ values are the means of the corresponding values in *c*. The curves are derived from the fits in *b*. For *a* and *b*, each point is the mean of two independent cultures, and each bar, which is smaller than the data symbol in some cases, denotes the range. For *c* and *d*, bars denote the errors associated with the nonlinear fits. For details of the analysis, see *SI Text*.

low magnesium (Fig. 1) is due to a corresponding plateau in the levels of PhoP-P as a function of [Mg^{2+}] (Fig. 4*c*). Interestingly, we have found that PhoP-regulated transcription is further activated in a PhoQ-dependent manner when cells are exposed to growth-limiting levels of Mg^{2+}, which are well below 10 μM (data not shown). There is considerable evidence that magnesium stimulation acts by direct interaction with PhoQ (10, 23–25, 28). The above results suggest this activation is not characterized by magnesium binding with a single dissociation constant. This is plausible given the multiple magnesium ions and multiple acidic residues in the PhoQ periplasmic domain that appear to be involved in this interaction (25).

For the above analysis, we have assumed for simplicity that each promoter binds a single PhoP-P molecule. However, the results can be easily extended to the case of binding by multiple PhoP-P molecules. For example, if PhoP-P binds promoters as a dimer, then the curves in Fig. 4 *b–d* remain unchanged provided the points corresponding to specific values of $[PhoP\text{-}P]_{effective}$ are now interpreted as values of $[PhoP\text{-}P]^2_{effective}$. For the general case of cooperative binding characterized by a Hill constant h, $[PhoP\text{-}P]_{effective}$ is replaced with $[PhoP\text{-}P]^h_{effective}$.

Concluding Remarks. We found that the relative responses of three PhoP-regulated promoters were identical over a remarkably large range of magnesium concentrations (Fig. 1*d*). Consistent with the predictions of a simplified model of transcriptional activation, differential regulation of these genes emerged at higher levels of PhoQ stimulus by treatment with the antimicrobial peptide LL-37 (Fig. 3*d*). Interestingly, even at the highest levels of stimulation, the promoters for *mgrB*, *hemL*, and *phoPQ* were apparently far from the maximal activity associated with saturated binding by PhoP-P (Fig. 4*b*). It is possible that maximal activity could be reached with different environmental conditions, such as the presence of other antimicrobial compounds or growth in much lower levels of magnesium. However, it is also possible that some PhoP-regulated promoters will remain far from saturation under all growth conditions. In this case, these promoters would be maximally responsive to changes in PhoQ activity for the range of PhoQ stimulation encountered by *E. coli* under physiological conditions.

Our results also highlight how stimulus–response curves, when measured with high precision, can be used to infer the parameters characterizing cell regulatory circuits *in situ*. This approach is complementary to *in vitro* biochemical measurements, which may be difficult to carry out in some cases and which may not always accurately reflect the conditions inside the cell, e.g., because of biochemical and biophysical differences between the *in vitro* and *in vivo* environments (29). Indeed, our results suggest that current *in vitro* measurements of PhoP binding to promoters do not accurately reflect the relative binding affinities *in vivo*. Importantly, we find that this cannot be simply explained by the absence of PhoP phosphorylation in the *in vitro* measurements, because we find that high-level expression of PhoP *in vivo* in the absence of phosphorylation shows the same ordering of promoter activation (SI Fig. 8). Our analysis, which is based on the steady-state behavior of the system, has some features in common with studies of activation kinetics of genetic circuits (30, 31). These approaches depend on assumptions concerning the physical, chemical, and biological mechanisms controlling gene expression *in vivo*. Therefore, the interpretation of our measurements must be viewed within this context. In particular, we assume that interactions of PhoP-P with regulatory sites at promoters can be described by a simple model of equilibrium binding, and that the extent of transcriptional activation is proportional to the fraction of bound PhoP-P at the promoter. These assumptions, which are simplifications of more accurate models of transcriptional regulation (e.g., ref. 32), are sufficient to account for the experimental measurements described here. Regardless of whether $[PhoP\text{-}P]_{effective}$ has a simple relationship to actual intracellular levels of PhoP-P, this parameter provides a unifying framework for analyzing and comparing PhoP-regulated promoters. This is evident from the excellent agree-

ment between the transcription data for PhoQ stimulation via low [Mg^{2+}] or LL-37 and the transcription curves determined independently from $PhoP_{ca}$ data (Fig. 4 *b* and *d*). Further studies with a larger range of stimuli, combined with precise kinetics measurements, will lead to a more refined model of the PhoQ–PhoP system and related regulatory circuits from *in situ* measurements.

Materials and Methods

Strains and Growth Conditions. All *E. coli* strains used in this study were derived from the K-12 strain MG1655 (33). A table of strains and plasmids with the details of their construction is given in *SI Text*.

Before each experiment, cells were grown overnight at 37°C in minimal A medium (34) containing 1 mM $MgSO_4$ and supplemented with 0.1% casamino acids and 0.2% glucose. Plasmids were maintained by using 50 μg/ml ampicillin. The pTrc-derived promoters were induced with isopropyl-β-D-thiogalactoside. For the data in Figs. 1 and 3 *b* and *c*, cultures were diluted 1:10^4 into prewarmed media with the level of $MgSO_4$ indicated in the figure and grown at 37°C for 3.5 h. We verified steady-state conditions were reached by measuring cellular fluorescence at several time points (data not shown). In experiments involving LL-37 and $PhoP_{ca}$ (Figs. 3*d* and 4, respectively), a dilution of 1:1,000 was used and cells were grown for 4.5 h. LL-37 was added after 3.5 h.

At appropriate times, cultures were cooled quickly in an ice-slurry, and streptomycin was added to 250 μg/ml to inhibit further translation. When necessary, cultures were centrifuged at 4°C and resuspended in $\approx$10 μl to concentrate the cells. Cellular fluorescence was measured by fluorescence microscopy as described previously (22). For further details, see *SI Text*.

We thank Andy Binns, Linda Kenney, Eleonora Garcia Vescovi, Carey Waldburger, Marjan van der Woude, Amy Vollmer, Jun Zhu, and members of the Binns, Zhu, and M.G. laboratories for helpful advice and discussions. This work was supported by National Science Foundation Grant MCB0212925 (to M.G.) and an American Heart Association predoctoral fellowship (to T.M.).

1. Kutsukake K, Ohya Y, Iino T (1990) *J Bacteriol* 172:741–747.
2. Kalir S, McClure J, Pabbaraju K, Southward C, Ronen M, Leibler S, Surette MG, Alon U (2001) *Science* 292:2080–2083.
3. Cotter PA, Jones AM (2003) *Trends Microbiol* 11:367–373.
4. Fujita M, Gonzalez-Pastor JE, Losick R (2005) *J Bacteriol* 187:1357–1368.
5. Waters CM, Bassler BL (2006) *Genes Dev* 20:2754–2767.
6. Groisman EA (2001) *J Bacteriol* 183:1835–1842.
7. Minagawa S, Ogasawara H, Kato A, Yamamoto K, Eguchi Y, Oshima T, Mori H, Ishihama A, Utsumi R (2003) *J Bacteriol* 185:3696–3702.
8. Zwir I, Shin D, Kato A, Nishino K, Latifi T, Solomon F, Hare JM, Huang H, Groisman EA (2005) *Proc Natl Acad Sci USA* 102:2862–2867.
9. Monsieurs P, De Keersmaecker S, Navarre WW, Bader MW, De Smet F, McClelland M, Fang FC, De Moor B, Vanderleyden J, Marchal K (2005) *J Mol Evol* 60:462–474.
10. Garcia Vescovi E, Soncini FC, Groisman EA (1996) *Cell* 84:165–174.
11. Soncini FC, Garcia Vescovi E, Solomon F, Groisman EA (1996) *J Bacteriol* 178:5092–5099.
12. Bader MW, Navarre WW, Shiau W, Nikaido H, Frye JG, McClelland M, Fang FC, Miller SI (2003) *Mol Microbiol* 50:219–230.
13. Bader MW, Sanowar S, Daley ME, Schneider AR, Cho U, Xu W, Klevit RE, Le Moual H, Miller SI (2005) *Cell* 122:461–472.
14. Soncini FC, Vescovi EG, Groisman EA (1995) *J Bacteriol* 177:4364–4371.
15. Ernst RK, Guina T, Miller SI (2001) *Microbes Infect* 3:1327–1334.
16. Brodsky IE, Gunn JS (2005) *Mol Interv* 5:335–337.
17. Shin D, Groisman EA (2005) *J Biol Chem* 280:4089–4094.
18. Kato A, Tanabe H, Utsumi R (1999) *J Bacteriol* 181:5516–5520.
19. Elowitz MB, Levine AJ, Siggia ED, Swain PS (2002) *Science* 297:1183–1186.
20. Ozbudak EM, Thattai M, Kurtser I, Grossman AD, van Oudenaarden A (2002) *Nat Genet* 31:69–73.
21. Batchelor E, Silhavy TJ, Goulian M (2004) *J Bacteriol* 186:7618–7625.
22. Miyashiro T, Goulian M (2007) *Methods Enzymol* 423:458–475.
23. Castelli ME, Garcia Vescovi E, Soncini FC (2000) *J Biol Chem* 275:22948–22954.
24. Chamnongpol S, Cromie M, Groisman EA (2003) *J Mol Biol* 325:795–807.
25. Cho US, Bader MW, Amaya MF, Daley ME, Klevit RE, Miller SI, Xu W (2006) *J Mol Biol* 356:1193–1206.
26. Cromie MJ, Shi Y, Latifi T, Groisman EA (2006) *Cell* 125:71–84.
27. Lejona S, Castelli ME, Cabeza ML, Kenney LJ, Garcia Vescovi E, Soncini FC (2004) *J Bacteriol* 186:2476–2480.
28. Montagne M, Martel A, Le Moual H (2001) *J Bacteriol* 183:1787–1791.
29. Bintu L, Buchler NE, Garcia HG, Gerland U, Hwa T, Kondev J, Kuhlman T, Phillips R (2005) *Curr Opin Genet Dev* 15:125–135.
30. Ronen M, Rosenberg R, Shraiman BI, Alon U (2002) *Proc Natl Acad Sci USA* 99:10555–10560.
31. Kalir S, Alon U (2004) *Cell* 117:713–720.
32. Bintu L, Buchler NE, Garcia HG, Gerland U, Hwa T, Kondev J, Phillips R (2005) *Curr Opin Genet Dev* 15:116–124.
33. Blattner FR, Plunkett G, 3rd, Bloch CA, Perna NT, Burland V, Riley M, Collado-Vides J, Glasner JD, Rode CK, Mayhew GF, *et al.* (1997) *Science* 277:1453–1474.
34. Miller JH (1992) *A Short Course in Bacterial Genetics: A Laboratory Manual and Handbook for Escherichia Coli and Related Bacteria* (Cold Spring Harbor Lab Press, Plainview, NY).